Folia Parasitologica

http://folia.paru.cas.cz

Research Article

Redescription of *Illiosentis cetratus* Van Cleave, 1945 (Acanthocephala: Illiosentidae) from *Menticirrhus undulatus* (Girard) in California, with notes on *Illiosentis furcatus* from Peru

Omar M. Amin[1] , **Anshu Chaudhary**[2] and **Hridaya S. Singh**[2,3]

[1] Institute of Parasitic Diseases, Scottsdale, Arizona, USA;

[2] Molecular Taxonomy Laboratory, Department of Zoology, Chaudhary Charan Singh University, Meerut (Uttar Pradesh), India;

[3] Maa Shakumbhari University, Saharanpur (Uttar Pradesh), India

Abstract: *Illiosentis* Van Cleave et Lincicome, 1939 initially included two species: *Illiosentis furcatus* Van Cleave et Lincicome, 1939 found in the West Atlantic from Cape Cod in Massachusetts, USA to northern Argentina and *Illiosentis cetratus* Van Cleave, 1945 with restricted distribution in the Pacific coast of southern California. We are reporting *I. furcatus* from Peru for the first time and describe a population of *I. cetratus* from the California corbina, *Menticirrhus undulatus* (Girard), from southern California. The proboscis hook formula was 14 longitudinal rows for *I. furcatus* of 18–23 hooks each compared to 16 rows of 19–24 hooks each reported by Van Cleave (1945). We complete the inadequate description of *I. cetratus* with new information on sexual differentiation in the length of the trunk, dorsal vs. ventral hooks, hook roots, trunk spines, two types of anterior recurved rooted hooks vs. posterior rootless straight hooks, measurements of dorsal and ventral hooks and spines, shape of hook roots, terminal position of the female gonopore, and of position of the cephalic ganglion at the anterior margin of the trunk. We also include new details of the reproductive system in both sexes including Saefftigen's pouch and cement gland ducts. We present new SEM and light microscope images. The Energy Dispersive X-ray analysis (EDXA) shows a high level of sulfur in anterior, middle and posterior hooks in various hook sites, as well as spectra of hook tips with a higher relative concentration of sulfur compared to other hook sites. For the placement of *I. cetratus*, phylogenetic analysis of sequences of three molecular markers, 18S, 28S rRNA and mitochondrial cox 1 genes, was performed with other related available sequences. The resulting analysis illustrated that *I. cetratus* was nested within a separate clade along with species of two genera, *Dentitruncus truttae* Sinzar, 1955 and *Neotegorhynchus cyprini* Lisitsyna, Xi, Orosová, Barčák et Oros, 2022 represented our species of *Illiosentis* separate from species of *Tegorhynchus* Van Cleave, 1921 (as also according to the morphology) with which the *Illiosentis* species were previously synonymised.

Keywords: redescription, EDXA, molecular profile, California corbina, SEM

The taxonomic history of the genus *Illiosentis* Van Cleave et Lincicome, 1939 is laden with changes, reassignments, and conflict. Van Cleave and Lincicome (1939) originally created the genus *Illiosentis* to accommodate *Illiosentis furcatus* Van Cleave et Lincicome, 1939 from the southern kingfish, *Menticirrhus americanus* (Linnaeus) (Sciaenidae), in the Gulf of Mexico off Grand Isle, Louisiana. It can be found in the West Atlantic from Cape Cod in Massachusetts, USA to northern Argentina. Shortly thereafter, Van Cleave (1945) described *Illiosentis cetratus* from the California corbina, *Menticirrhus undulatus* (Girard). These two species remained the only known species of *Illiosentis* for a while, as recognised by Petrochenko (1956) and Yamaguti (1963).

Petrochenko (1956) created a key to the species distinguished by their proboscis hook number and arrangement but *I. furcatus* and *I. cetratus* remained the two most closely related species to each other compared to all currently known species of the genus. More species of *Illiosentis* were beginning to be recognised from other parts of the world by then. Yamaguti (1963) noted that Golvan (1960) proposed *Illiosentis edmondsi* Golvan, 1960 nom. nov. for *I. furcatus* of Edmonds, 1957 from Australia. Golvan (1955) additionally described *Illiosentis africanus* (= *Illiosentis furcatus africanus* Golvan, 1955) from Senegal.

These were the four species recognised by Golvan (1969) who later on (Golvan 1994) added *Illiosentis multacanthus* Mamaev, 1970 from the Gulf of Tonkin, Vietnam. *Illiosentis heteracanthus* Cable et Linderoth, 1963 from West Indies, Curaçao, South Caicos, Turks, and Caicos Islands was also added but was emended by Monks and Pullido-Flores (2002).

There are 12 known genera in Illiosentidae (see Amin 2013) with six recognisable species of *Illiosentis* to date (above). In the interim, many relegations and reassignments have taken place, the most important of which are those by Bullock and Mateo (1970), Amin (1985, 2013). Amin (1985, 2013) transferred all known species of *Illiosentis* with *Tegorhynchus* Van Cleave, 1921 based on Bullock and Mateo's (1970) research on type specimens of species known then. Bullock and Mateo (1970) stated that they were "convinced that *Illiosentis* and *Tegorhynchus* are congeneric. All species are therefore, assigned to *Tegorhynchus* (family Tegorhynchidae)."

We have since changed our position after examining Monks and Pullido-Flores (2002) who resurrected *Illiosentis*. They convincingly argued (p. 365) that "the 2 genera differ in that the proboscis of members of *Illiosentis* have ventral hooks in the posterior-most circle that are greatly enlarged and male worms have a heavy muscular sheath covering the urogenital duct, both of which are absent in members of *Tegorhynchus*." The distinction was clearly made between the posterior-most proboscis hooks being part of the basal hook ring or in a ventral crescent far from basal hooks.

Additionally, Golvan (1994, p 161) did not accept that "*I. furcatus* Van Cleave et Lincicome, 1939 (type species) (Louisiana, USA): may be a *Tegorhynchus* (fide Buckner and Mateo 1978; meaning Bullock and Mateo 1970); this synonymy cannot be accepted because in the genus *Illiosentis*, there are 2 "lips" surrounding the female genital pore and those structures are absent in the genus *Tegorhynchus* (vide Leotta et al. 1982)." Most recently, and in agreement with our present position, Lisitsyna et al. (2022), in erecting their new genus *Neotegorhynchus* Lisitsyna, Xi, Orosová, Barčák et Oros, 2022 (Illiosentidae), recognised each of *Illiosentis* and *Tegorhynchus* independently as a valid genus.

A number of other reassignments were made, mostly by Golvan (1994). These included transferring *Illiosentis ctenorhynchus* Cable et Linderoth, 1963 and *Illiosentis longispinus* Cable et Linderoth, 1963 to *Dollfusentis* Golvan, 1969 by Golvan (1969) as *Dollfusentis ctenorhynchus* and *Dollfusentis longispinus*. The turbulent history of the genus *Illiosentis* did not end there. We, however, decided to shed some more light on the more recent collections of *I. cetratus* and provide a new perspective of its morphology using SEM, biochemistry of hooks using Energy Dispersive X-ray Analysis (EDXA), and molecular analysis for the first time.

The morphological aspects covered by Van Cleave (1945) were greatly lacking in anatomical details that a redescription of the species was necessitated. Our treatment included the many morphological features missed by Van Cleave (1945) that we present in our redescription and supplemented by a generous collection of SEM images complimenting the images lacking in the original description and introducing new features never before mentioned. A small collection of *I. furcatus* from Peru gave new perspectives of its morphology. We also elucidate the phylogenetic position of *I. cetratus* based on nucleotide sequence data of 18S, 28S rRNA and cox1 genes to assess its taxonomic position.

MATERIALS AND METHODS

Collections

About 50 adult specimens of *Illiosentis cetratus* were collected from the California corbina *Menticirrhus undulatus* in Redondo Beach, California (33.8580, -118.3789) in July, September, and November 2017. Freshly collected specimens were placed in water and refrigerated for 2–3 days before fixing in cold 70% ethanol. Twenty-two specimens were processed for parasitological examination, eight for SEM, and 11 for molecular analysis of which two were used. The remaining nine specimens are in the senior author's collection. Two specimens of *Illiosentis furcatus* (one male, one female) were collected from a Lorna drum, *Sciaena deliciosa* (Tschudi) from La Punta (Callao), Lima, Peru (-12.0713, -77.1625) in 1988.

Processing for morphological studies

Worms were punctured with a fine needle and subsequently stained in Mayer's acid carmine, destained in 4% hydrochloric acid in 70% ethanol, dehydrated in ascending concentrations of ethanol (24 hr each), and cleared in 100% xylene, then in 50% Canada balsam and 50% xylene (24 hr each). Whole worms were then mounted in Canada balsam. Measurements are in micrometres, unless otherwise noted; the range is followed by the mean values between parentheses. Width measurements represent maximum width. Trunk length does not include proboscis, neck, or bursa.

Optical microscope images

Optical microscope images were acquired using a BH2 light Olympus microscope (Olympus Optical Co., Osachi-shibamiya, Okaya, Nagano, Japan) attached to an AmScope 1000 video camera (United Scope LLC, dba AmScope, Irvine, California, USA), linked to an ASUS laptop equipped with HDMI high-definition multimedia interface system (Taiwan-USA, Fremont, California). Images from the microscope were transferred from the laptop to a USB and stored for subsequent processing on a computer.

Scanning electron microscopy (SEM)

Eight specimens that had been fixed and stored in 70% ethanol were processed for SEM following standard methods (Lee 1992). This included critical point drying (CPD) (Tousimis Automandri 931.GL) and mounting on aluminum SEM sample mounts (stubs) using conductive double-sided carbon tape. Samples were sputter coated with an 4 : 1 gold-palladium target for three minutes using a sputter coater (Quorum – Q150T ES) equipped with a planetary stage, depositing an approximate thickness of 20 nm. Samples were placed and observed in an FEI Helios Dual Beam Nanolab 600 (FEI, Hillsboro, Oregon) scanning electron microscope with digital images obtained in the Nanolab software (FEI). Samples were imaged using an accelerating voltage of 5 kV, and a probe current of 86 pA, at high vacuum using a GSE detector.

Focused Ion Beam (FIB) sectioning of hooks

A dual-beam SEM with gallium (Ga) ion source (GIS) is used for the LIMS (Liquid Ion Metal Source) part of the process. The gallium beam (LIMS) is a gas injection magnetron sputtering

technique whereby the rate of cutting can be regulated. The hooks were sectioned at two positions (tip and middle) using the FEI Helios Dual Beam Nanolab mentioned above. The dual-beam FIB/SEM is equipped with a gallium (Ga) Liquid Ion Metal Source (LIMS). The hooks of the acanthocephalans were centred on the SEM stage and cross-sectioned using an ion accelerating voltage of 30 kV and a probe current of 2.7 nA following the initial cut. The time of cutting is based on the nature and sensitivity of the tissue. The sample also goes through a cleaning cross-section milling process to obtain a smoother surface. The cut was analysed with an X-ray usually at the tip, middle, and base of hooks for chemical ions with an electron beam (Tungsten) to obtain an X-ray spectrum. The intensity of the GIS was variable according to the nature of the material being cut. Results were stored with the attached imaging software, then transferred to a USB for future use.

Energy Dispersive X-ray analysis (EDXA)

The Helios Nanolab 600 is equipped with an EDXA (Mahwah, New Jersey) TEAM Pegasus system with an Octane Plus detector. The sectioned cuts were analysed by EDXA. Spectra of selected areas were collected from the centre and the edge of each cross-section. EDXA spectra were collected using an accelerating voltage of 15 kV, and a probe current of 1.4 nA. Data collected included images of the displayed spectra as well as the raw collected data. Relative elemental percentages were generated by the TEAM software.

Molecular methods

Genomic DNA was extracted from two specimens using QIAGEN DNeasy™ tissue kit (Qiagen, Hilden, Germany), according to the manufacturer's recommendations. The partial 18S rDNA region was amplified by polymerase chain reaction (PCR) using the primers 18SU467F (forward, 5'-ATCCAAGGAAGGCAG-CAGGC-3'); 18SL1310R (reverse, 5'-CTCCACCAACTAA-GAACGGC-3') (Suzuki et al. 2008) while the 28S rRNA gene was amplified using the primers, forward, 5'-CTAAGGAGT-GTGTAACAACTCACC-3', reverse, 5'-AATGACGAGGCAT-TTGGCTACCTT-3') and forward, 5'-GATCCGTAACTTCGG-GAAAA-3', reverse, 5'-CTTCGCAATGATAGGAAGAGCC-3' (García-Varela and Nadler 2005). Primers used for the amplification of mitochondrial cytochrome oxidase c subunit 1 gene (cox1) were LCO1490 (5'-GGTCAACAAATCATAAAGATATTGG-3') and HC02198 (5'-TAAACTTCAGGGTGACCAAAAAAT-CA-3') (Folmer et al. 1994).

Polymerase chain reactions were performed in 25 μl reactions, containing 1 μl of each primer, 2.5 μl of 10 × buffer including MgCl$_2$, 3 μl of dNTPs (10 mM), 0.9 μl of 1 U of Taq DNA polymerase (Biotools, Madrid, Spain) with a final concentration of 10 pMol, 3 μl of the genomic DNA and 13.6 μl of distilled water. For 18S rDNA and cox1 regions, the thermocycling protocol followed Amin et al. (2022) and for 28S gene the thermocycling profile was followed according to García-Varela and Nadler (2005). PCR products were checked after electrophoresis on a 1.5% agarose in TAE gel under UV transilluminator. PCR amplicons were purified with Purelink™ Quick Gel Extraction and PCR Purification Combo Kit (Invitrogen, Löhne, Germany). Sequencing reactions were performed using ABI Big Dye v.3.1 (Applied Biosystems, Foster City, California) according to the manufacturer's protocol with the above-mentioned primers.

Sequences generated during the study from both strands were checked and edited using the software MEGA 11 (Tamura et al. 2021). A comparison for similarities of 18S, 28S and cox1 sequences with sequences from the GenBank database was executed using the BLAST search (http://www.ncbi.nlm.nih.gov/BLAST). The 18S, 28S rDNA and cox 1 sequence alignments were analysed independently and as well as in a combined dataset. For the phylogenetic relationships, the nucleotide sequences were aligned using the CLUSTAL W algorithm in MEGA 11 (Tamura et al. 2021). The genetic divergence among isolates studied in the present study was estimated using the uncorrected (p-distance) method for 18S rDNA and cox1 gene. For the selection of nucleotide substitution model for each molecular marker, jModelTest version 2.1.7 (Darriba et al. 2012) was used and applying the Akaike criterion the best nucleotide substitution model was found GTR + G + I.

Phylogenetic trees were constructed through Maximum likelihood (ML) with the software MEGA 11 (Tamura et al. 2021) and Bayesian inference (BI) method with the program Topali 2.5 (Milne et al. 2008), respectively. For ML analysis, 10,000 bootstrap replicates were run to assess nodal support. For BI trees, with two runs of the Markov chain (MCMC) for 10 million generations, sampled every 1,000 generations and the first 25% of the sampled trees were discarded as 'burn-in'. Newly generated sequences of *I. cetratus* were aligned with available sequences from the GenBank database of related members, including other sequences that were used as out groups for rooting the trees.

RESULTS

Our specimens of *Illiosentis cetratus* were collected from the California corbina, *Menticirrhus undulatus*, in the southern California Pacific coast where the host distribution is restricted. In addition, we collected two specimens of *Illiosentis furcatus* (1 male, 1 female) from a Lorna drum, *Sciaena deliciosa*, off Lima, Peru in 1988.

Redescription of *Illiosentis cetratus* Van Cleave, 1945

General (Figs 1–6). With essential characteristics of *Illiosentis* as originally diagnosed by Van Cleave and Lincicome (1939). Worms long, slender, cylindrical, slightly wider at anterior third and at posterior end. Anterior and posterior trunk regions with corresponding electron dense micropores (Fig. 3D,E). Sexual dimorphism in length of trunk, dorsal vs. ventral proboscis hooks and trunk spines. Posterior extremity of females with dorsal protuberance (Fig. 4D,E). Trunk spines (13–15) in one zone with one continuous ring anteriorly (Fig. 2C–E), more numerous in females than in males, ventrally than dorsally (Fig. 2F), and larger anteriorly than posteriorly (Table 3), with core rods (Fig. 5E). Sensory papillae between hooks 7–9 from posterior (Figs 1A, 5C) and on various trunk locations (Figs 2E, 3F, 4C,D).

Proboscis long, club-shaped, with small apical organ not apparent externally (Fig. 1B), and usually 14 longitudinal rows of 18–23 hooks each. Hooks with cortical serration (Fig. 1D), of 2 types: 10–13 anterior hooks with strongly curved blades (Fig. 1C,E,F) and slightly shorter roots with

Table 1. Length of dorsal and ventral proboscis hooks and roots of five males of *Illiosentis cetratus* Van Cleave, 1945 with 21 hooks in a longitudinal row each from *Menticirrus undulatus* (Girard) in California.

Hook no.	Dorsal hook length	Ventral hook length	Dorsal root length	Ventral root length
1	32–57 (44)*	45–58 (49)	25–30 (27)	37–50 (45)
2	47–72 (57)	55–83 (65)	33–62 (51)	48–63 (56)
3	55–75 (66)	70–92 (71)	53–75 (63)	65–78 (71)
4	68–83 (73)	75–90 (78)	55–75 (63)	60–80 (71)
5	63–82 (71)	68–85 (75)	50–67 (59)	63–77 (70)
6	62–82 (69)	63–80 (71)	50–65 (58)	60–75 (63)
7	60–77 (67)	63–80 (70)	43–65 (52)	55–62 (58)
8	58–77 (64)	60–80 (68)	42–63 (51)	55–62 (58)
9	55–72 (62)	60–75 (67)	38–60 (48)	50–60 (57)
10	50–71 (56)	45–75 (60)	40–50 (45)	50–57 (55)
11	35–62 (49)	50–67 (60)	36–50 (41)	40–50 (45)
12	35–50 (42)	38–55 (51)	35–50 (41)	40–52 (46)
13	28–44 (36)	32–50 (38)	---**	---
14	28–44 (36)	33–50 (38)	---	---
15	28–43 (34)	33–50 (39)	---	---
16	28–42 (36)	32–55 (41)	---	---
17	28–42 (34)	38–55 (46)	---	---
18	28–35 (34)	38–55 (45)	---	---
19	28–38 (34)	42–55 (45)	---	---
20	28–38 (35)	40–55 (49)	---	---
21	33–45 (41)	55–78 (62)	---	---

*Range (mean) in micrometres

**Posterior 9 hooks are rootless

Table 2. Length of dorsal and ventral proboscis hooks and roots of five females of *Illiosentis cetratus* Van Cleave, 1945 with 21 hooks in a longitudinal row each from *Menticirrus undulatus* (Girard) in California.

Hook no.	Dorsal hook length	Ventral hook length	Dorsal root length	Ventral root length
1	45–52 (50)*	50–60 (55)	32–40 (37)	38–50 (43)
2	65–72 (67)	68–78 (71)	50–60 (54)	52–58 (55)
3	75–85 (81)	75–84 (81)	60–67 (62)	58–70 (65)
4	75–85 (83)	78–88 (83)	55–70 (63)	58–78 (68)
5	75–87 (80)	68–88 (81)	55–70 (63)	55–75 (65)
6	75–82 (77)	78–85 (80)	44–65 (57)	50–70 (62)
7	72–80 (75)	72–82 (77)	42–62 (54)	50–65 (59)
8	64–80 (73)	73–82 (77)	42–57 (50)	50–65 (57)
9	60–77 (71)	73–85 (77)	40–50 (46)	48–60 (55)
10	52–72 (67)	63–80 (73)	40–50 (45)	48–60 (53)
11	47–65 (57)	53–73 (65)	37–47 (41)	43–55 (47)
12	42–50 (46)	44–65 (54)	37–42 (38)	37–50 (41)
13	37–52 (47)	45–60 (50)	---**	---
14	40–50 (45)	42–55 (48)	---	---
15	39–47 (43)	42–52 (48)	---	---
16	38–45 (41)	42–48 (44)	---	---
17	38–45 (41)	38–52 (45)	---	---
18	40–47 (43)	45–55 (47)	---	---
19	40–50 (42)	42–60 (51)	---	---
20	42–50 (44)	50–62 (56)	---	---
21	43–55 (48)	65–75 (73)	---	---

*Range (mean) in micrometres.

**Posterior 9 hooks are rootless.

small anterior manubrial (Figs 1F, 5A), and 8–10 posterior spine-like rootless hooks (Figs 2A, 5B). Ventral hooks and roots invariably larger than dorsal hooks and roots. Apical hooks small, increasing to maximum size at 4th position from anterior, gradually decreasing at posterior-most position. Posterior rootless hooks smaller, more crowded, with comparable size (Fig. 2A) but becoming larger posteriorly reaching maximum basally on ventral side (Figs 2B, 5B, Tables 1, 2). Neck prominent. Proboscis receptacle double-walled, about twice as long as proboscis with cephalic ganglion near its anterior end just posterior to anterior trunk extremity (Fig. 5D). Lemnisci digitiform, unequal, markedly longer than receptacle.

Males (based on 10 mature specimens with sperm). Trunk 15.6–21.3 (18.3) mm long by 0.52–0.87 (0.72) mm wide anteriorly. Proboscis 0.95–1.25 (1.17) mm long by 0.24–0.27 (0.26) mm wide anteriorly, usually with 14 (rarely 13, 15 or 16 in single males) rows of 18–23 hooks each. Measurements of 12 dorsal and ventral anterior rooted hooks and 9 spine-like posterior hooks in males with 21 hooks per row and measurements of slightly smaller roots of anterior hooks in Table 1. Neck 250–400 (332) long dorsally by 175–225 (207) wide at base. Trunk with 10–15 dorsal and 15–20 ventral spines (see Table 3 for measurements). Proboscis receptacle 2.20–2.90 (2.57) mm long by 0.25–0.35 (0.30) wide. Short lemnisci 3.25–4.62 (3.97) mm long by 0.10–0.15 (0.12) mm wide. Long lemnisci 3.95–6.00 (4.72) mm long by 0.10–0.15 (0.12) mm wide. Testes postequatorial in posterior fourth of trunk with no space separating reproductive structures. Anterior testis wider anteriorly and larger than posterior testis, 1.00–1.55 (1.26) mm long by 0.22–0.35 (0.27) mm wide anteriorly. Posterior testis 0.87–1.17 (0.99) mm long by

0.22–0.32 (0.28) wide. Cement glands bulbous and stagger anteriorly (Fig. 6A) and continuous with cement ducts posteriorly. Smallest glands 0.62–1.25 (0.90) mm long by 0.14–0.20 (0.16) mm wide anteriorly and longest glands 0.92–1.65 (1.38) mm long by 0.17–0.27 (0.23) mm wide anteriorly. Saefftigen's pouch club-shaped, dorsal (Fig. 6B) 1.12–1.75 (1.43) mm long by 0.20–0.35 (0.27) mm wide anteriorly. Sperm vesicle (Fig. 6C) somewhat rectangular, at posterior end of system, 500–675 (606) long by 225–325 (277) wide. Bursa thick with constriction at distal end (Fig. 4A) bearing large occasional sensory papillae (Fig. 4B,C), 0.77–1.10 (0.94) mm long by 0.62–1.00 (0.78) mm wide. Circles of round sensory papillae on the inner margin of bursa (Fig. 4C). Ducts of dorsal Saefftigen's pouch, sperm vesicle, and cement gland ducts pool into bursa near penis (Fig. 6C).

Females (based on 12 mature specimens with eggs). Trunk 21.3–30.7 (25.3) mm long by 0.52–0.87 (0.71) mm wide. Proboscis 1.20–1.50 (1.34) mm long by 0.26–0.35 (0.31) mm wide anteriorly, usually with 14 (15 in one specimen) (14) rows of 20–23 (21) hooks each. Measurements of 12 dorsal and ventral anterior rooted hooks and 9 spine-like posterior hooks in females with 21 hooks per row and measurements of slightly smaller roots of anterior hooks in Table 2. Neck 250–450 (384) long dorsally by 225–275 (240) wide at base. Trunk with 17 dorsal spines (18, 19, 20, 21 spines in 1 single specimen each) and 20 ventral spines (21 spines in single specimen); see Table 3 for measurements. Proboscis receptacle 2.50–3.30 (2.87) mm long by 0.27–0.35 (0.32) mm wide. Short lemnisci 3.95–5.00 (4.40) mm long by 0.08–0.12 (0.10) wide. Long lemnisci 3.95–5.35 (4.65) mm long by 0.12–0.14 (0.13) mm wide. Reproductive system 832–957 (881) long (3.5%
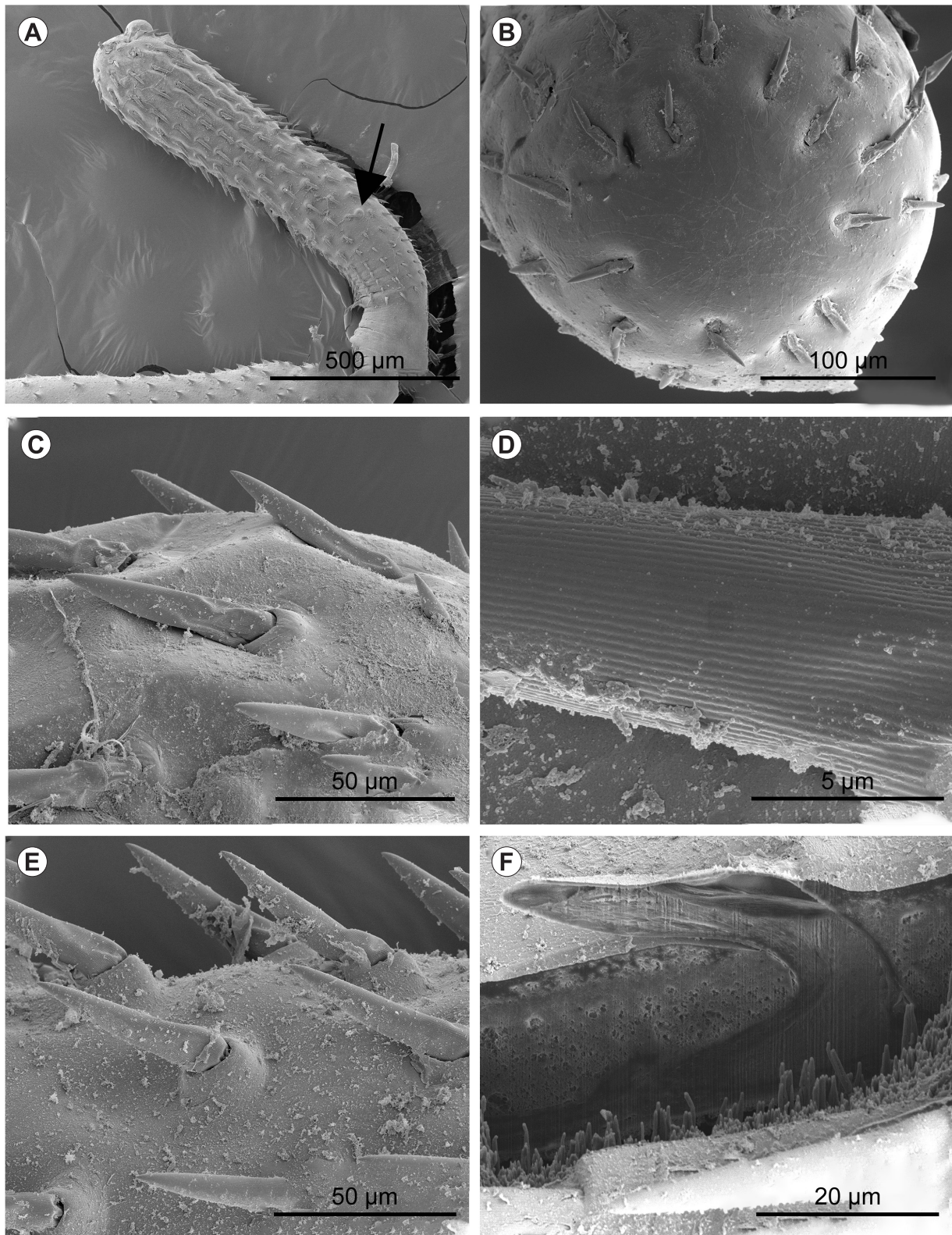
Fig. 1. SEM of specimens of *Illiosentis cetratus* Van Cleave, 1945 from *Menticirrhus undulatus* (Girard) in California. **A** – proboscis of a female specimen showing the crowded smaller posterior hooks and the round sensory papilla at hook no. 7 from posterior (arrow). Note the curvature of the neck creating the usual ventral orientation of the proboscis; **B** – the apical surface of a proboscis of a male specimen showing the pattern of hook rows and the apparent lack of apical organ; **C** – apical (far right) and sub-apical anterior hooks of a female specimen; **D** – a higher magnification of an anterior hook from Fig. 1C detailing the pattern of cortical serration characteristic of all hooks of this species; **E** – a series of middle rooted hooks on the proboscis of a female specimen; **F** – a Gallium-cut longitudinal section of a middle hook showing the prominent posteriorly directed simple root and the arrangement of the subtegumental layer of the proboscis wall. Small anterior root manubrium is obscured.
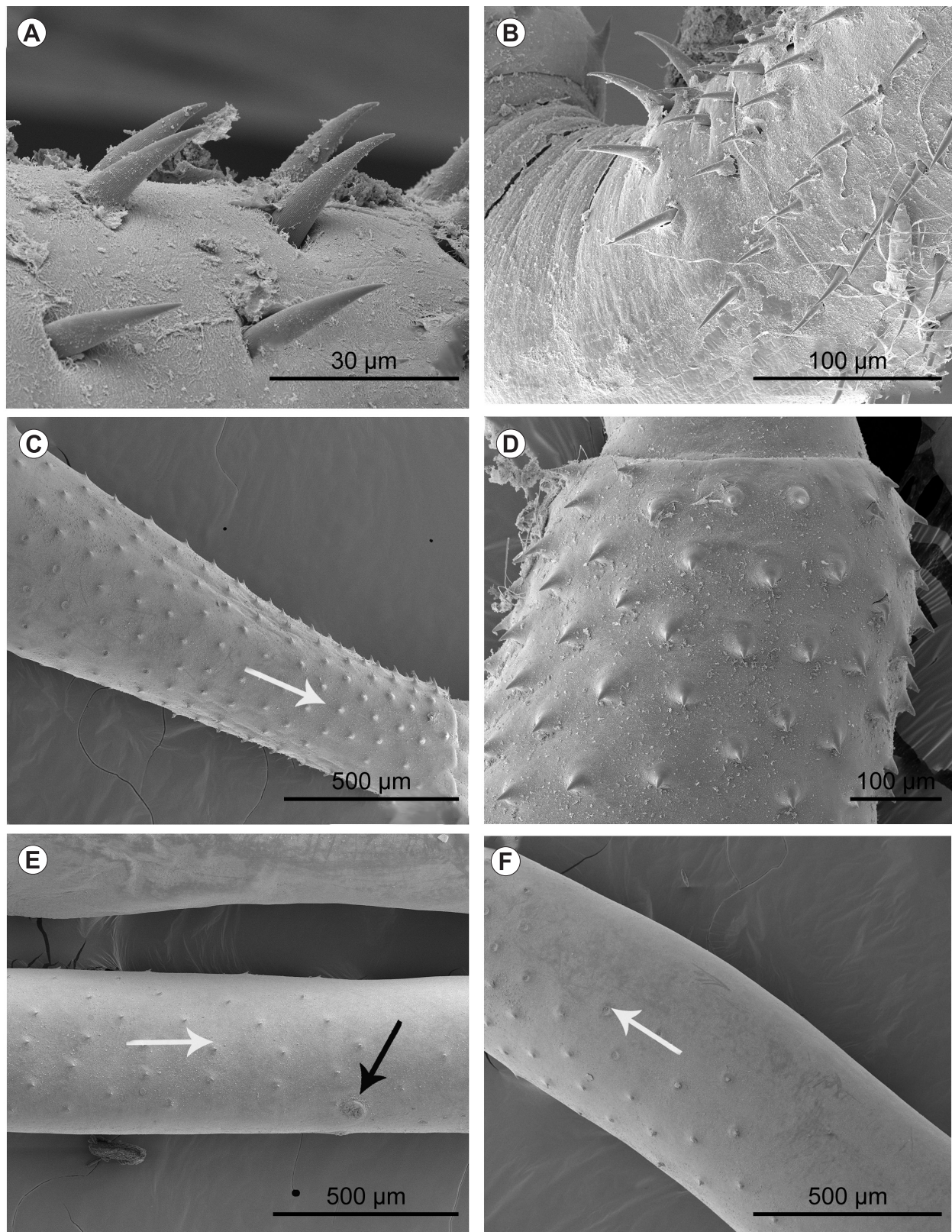
Fig. 2. SEM of specimens of *Illiosentis cetratus* Van Cleave, 1945 from *Menticirrhus undulatus* (Girard) in California. **A** – a few crowded posterior hooks of a female specimen showing the characteristic cortical serration; **B** – the posterior part of the proboscis of a male specimen showing the differentially enlarged ventral basal hooks (top left) compared to the lateral and dorsolateral hooks; **C** – the anterior trunk of a female specimen showing the distribution of spines in irregular circles (or rows). Arrow points to anterior end. Some spines at lower left are broken off; **D** – a higher magnification of anterior trunk spines showing the anterior-most spines to be in a relatively regular circle with the exception of the odd spine closer to the neck. The irregularity of the other circles of spines is apparent; **E** – irregular posterior trunk spines of a female specimen showing one of the occasional sensory papillae (black arrow). White arrow points to anterior end; **F** – posterior trunk spines in a female specimen showing fewer spines dorsally and more spines ventrally (arrow points to anterior end).
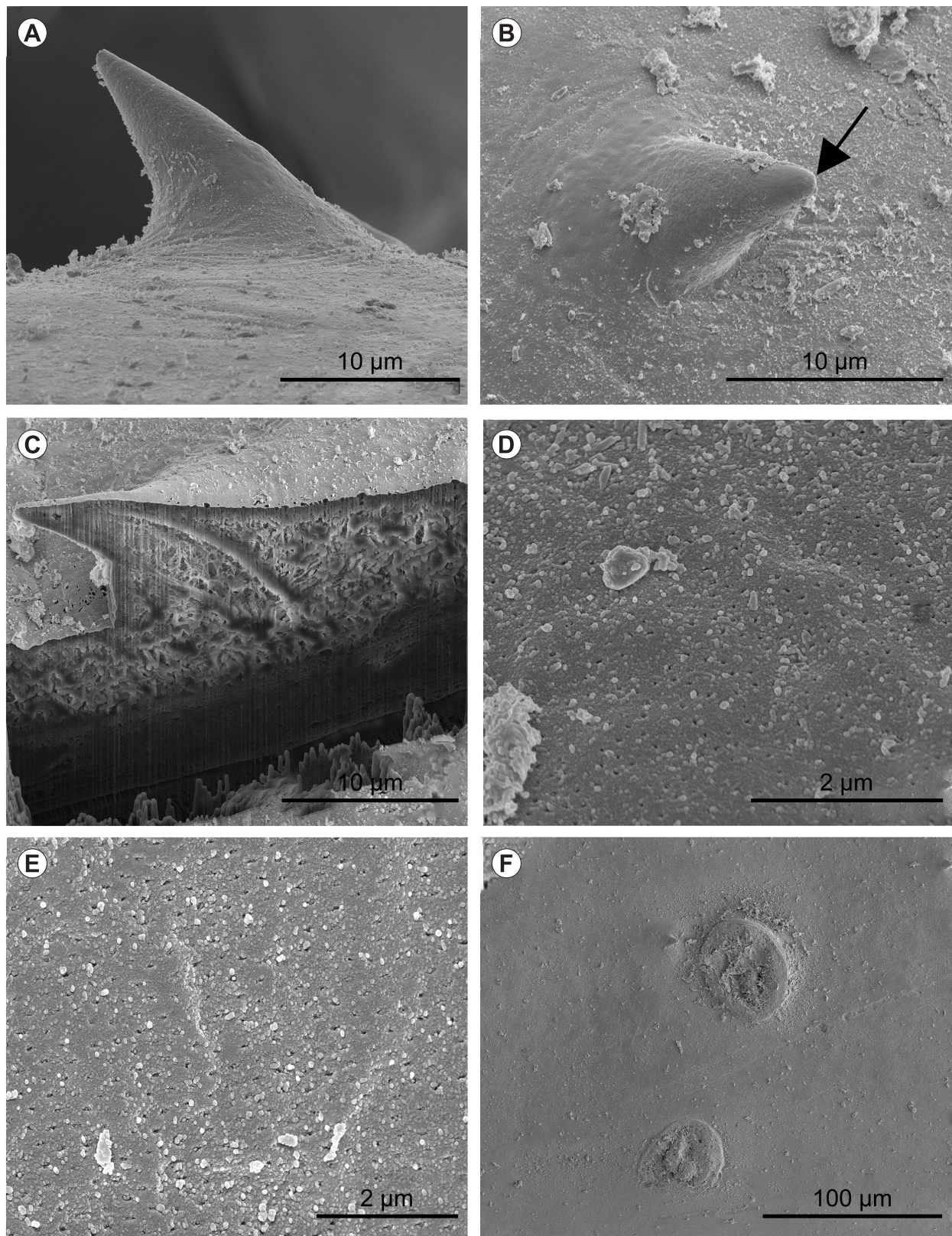
Fig. 3. SEM of specimens of *Illiosentis cetratus* Van Cleave, 1945 from *Menticirrus undulatus* (Girard) in California; **A** – lateral view of a trunk spine showing its broad base and posteriorly-directed tip in a female specimen; **B** – an apical view of the same spine in Fig. 3A showing the extension of micropores on its cortical layer (except the distal end) as in the tegumental layer of the body wall. Note the lack of hollowed apical end (arrow) sometimes found in trunk spines of other acanthocephalan species; **C** – a Gallium-cut section of a spine showing its internal structure blending with the structure of the sub-tegumental body wall layer; **D, E** – differential distribution of micropores in the anterior and posterior trunk integument, respectively; **F** – different types of sensory structures in the posterior spiny area of a female specimen.

Table 3. Length of dorsal and ventral trunk spines of five males and 5 females of *Illiosentis cetratus* Van Cleave, 1945 from *Menticirrus undulatus* (Girard) in California.

Spine no.	Males		Females	
	Dorsal spine length	Ventral spine length	Dorsal spine length	Ventral spine length
1	22–32 (25)*	22–30 (27)	21–32 (27)	30–38 (33)
2	22–30 (26)	25–32 (27)	25–27 (26)	30–35 (33)
3	22–30 (26)	22–32 (25)	25–30 (26)	28–38 (32)
4	22–32 (26)	20–32 (25)	20–27 (24)	28–42 (32)
5	20–30 (24)	20–30 (24)	25–30 (26)	28–35 (31)
6	18–28 (24)	20–30 (24)	25–27 (25)	20–30 (26)
7	20–32 (26)	20–30 (24)	25–27 (25)	28–33 (30)
8	20–30 (25)	20–25 (23)	25–27 (26)	25–35 (31)
9	20–30 (24)	18–25 (22)	25–27 (26)	25–28 (27)
10	17–30 (22)	18–28 (24)	20–26 (24)	25–33 (28)
11	17–25 (20)	18–25 (21)	23–25 (24)	23–33 (27)
12	10–18 (15)	18–25 (22)	15–23 (19)	25–31 (26)
13	15	18–27 (22)	15–27 (21)	23–28 (25)
14	15	18–25 (21)	17–27 (21)	20–30 (25)
15	18	15–25 (19)	17–25 (20)	18–30 (24)
16	---	18–20 (19)	17–27 (22)	20–28 (33)
17	---	22	17–25 (21)	18–33 (26)
18	---	20	27	20–25 (22)
19	---	18	23	22–28 (25)
20	---	12	20	22–25 (23)
21	---	---	23	25

*Range (mean) in micrometres.

of trunk length). Distal part of vagina tubular, enveloped in thick smooth muscular wall. Uterine bell funnel-shaped with thick lobulated wall and few uterine bell cells. Posterior-most tip of trunk with large paravaginal fan-shaped muscle (Fig. 6D). Gonopore at narrowing terminal end of trunk well posterior to dorsal protuberance (Fig. 6D). Eggs oblong with barely visible circular ring pattern (Fig. 4F) and marked polar prolongation of fertilisation membrane (Fig. 5F), 60–78 (69) long by 13–18 (16) in diameter.

Taxonomic summary

Type and current host: California corbina, *Menticirrhus undulatus* (Girard).

Type locality: Pacific coast at La Jolla, California (33.8581, -118.3789). Additional locality: Pacific coast at Redondo Beach, California (33.8580, -118.3789).

Site of infection: Intestine.

Materials deposited: Harold W. Manter Laboratory (HWML) collection no. 226780 (seven specimens, designated as neotypes, on five slides).

Representative DNA sequence: The newly generated sequences were deposited in GenBank under the following accession numbers: 18S rDNA: ON180690 (879 bp), ON180689 (838 bp); 28S rDNA: OR166369 (1075 bp), OR166425 (1025 bp); cox1: ON184031 (589 bp), ON184030 (583 bp).

Remarks

Despite the incomplete original description of *I. cetratus* from the corbina, *M. undulatus*, and the absence of measurements of practically all structures, except for the trunk, eggs, proboscis, and a few occasional hooks, we were able to clearly identify our specimens as *I. cetratus*. Van Cleave's (1945) line drawings (figs. 1–3) of two pro-

boscides (1 with 21–23 hooks per row and the other with 20) and a male reproductive system were the basis for the comparison. His type specimens in his personal collection in Urbana, Illinois were not available for examination. Similarities with the original description included comparability of the male reproductive system (his fig. 1) and the female reproductive system with dorsal protuberance and fan-shaped muscle, egg size (58–72 × 8–12 μm compared to 62–78 × 13–18 μm in our specimens). The female reproductive system is comparable to that of *I. furcatus* as stated by Van Cleave and Lincicome (1939 – their fig. 4, p. 417) except for the absence of genital spines characteristic of *I. furcatus* which is a species-specific trait.

Our specimens of *I. cetratus* differ from those described by Van Cleave (1945) in the hook formula and the position of its sensory papillae. While the number of hooks per row was similar, the proboscis in our specimens of *I. cetratus* had mostly 14 longitudinal rows which is the typical number of rows in the proboscis of *I. furcatus*. This can pose a serious taxonomic issue. Van Cleave (1945) also reported lateral papillae "at the level of from 8–14 hooks from posterior extremity of proboscis" (at level of hook 11 in his fig. 2, p. 58) but the papillae in our specimens were at the level of 7–9 hooks from posterior extremity. These may all be interpreted as population-related variations but the fact that our specimens and his were collected from the same host species and at very close localities in California, casts doubts about the accuracy of the original description.

Van Cleave (1945) was apparently unable to identify and locate the cephalic ganglion. We detected it at the anterior end of the proboscis receptacle just posterior to the level of the anterior extremity of the trunk (Fig. 5D). In *I. furcatus*, it was clearly identified and labelled at the ventral interface of the receptacle with the posterior proboscis (fig. 2 of Van Cleave and Lincicome, 1939). In *I. cetratus*, Van Cleave (1945) made no reference to the two types of hooks, their dorsoventral differentiation or to the roots, and gave no complete measurements of either. He did not provide complete measurements or counts of dorsal and ventral trunk spines except to mention (p. 58) "body spines numerous, restricted to a single uninterrupted zone at the anterior end of the body; commonly 38–42 μ in length."

Micropores

The trunk had apparent osmiophilic micropores of various diameters, shapes and distribution in various parts (Fig. 3D,E). In some areas, the micropores were more widely spaced than in others.

**Energy Dispersive X-ray Analysis (EDXA)**

The EDXA describes the elemental content of hooks delineating the hardening elements characteristic of each acanthocephalan species. The EDXA results of the hook sections (Tables 4, 5; Figs. 7, 8) of *I. cetratus* show a high level of sulfur in anterior, middle and posterior hooks in various hook sites. The EDXA spectra of the tip of the hooks showed a higher relative concentration of sulfur compared to other hook sites. The spectra of the tip of the mid-hook showed the highest sulfur compared to the centre
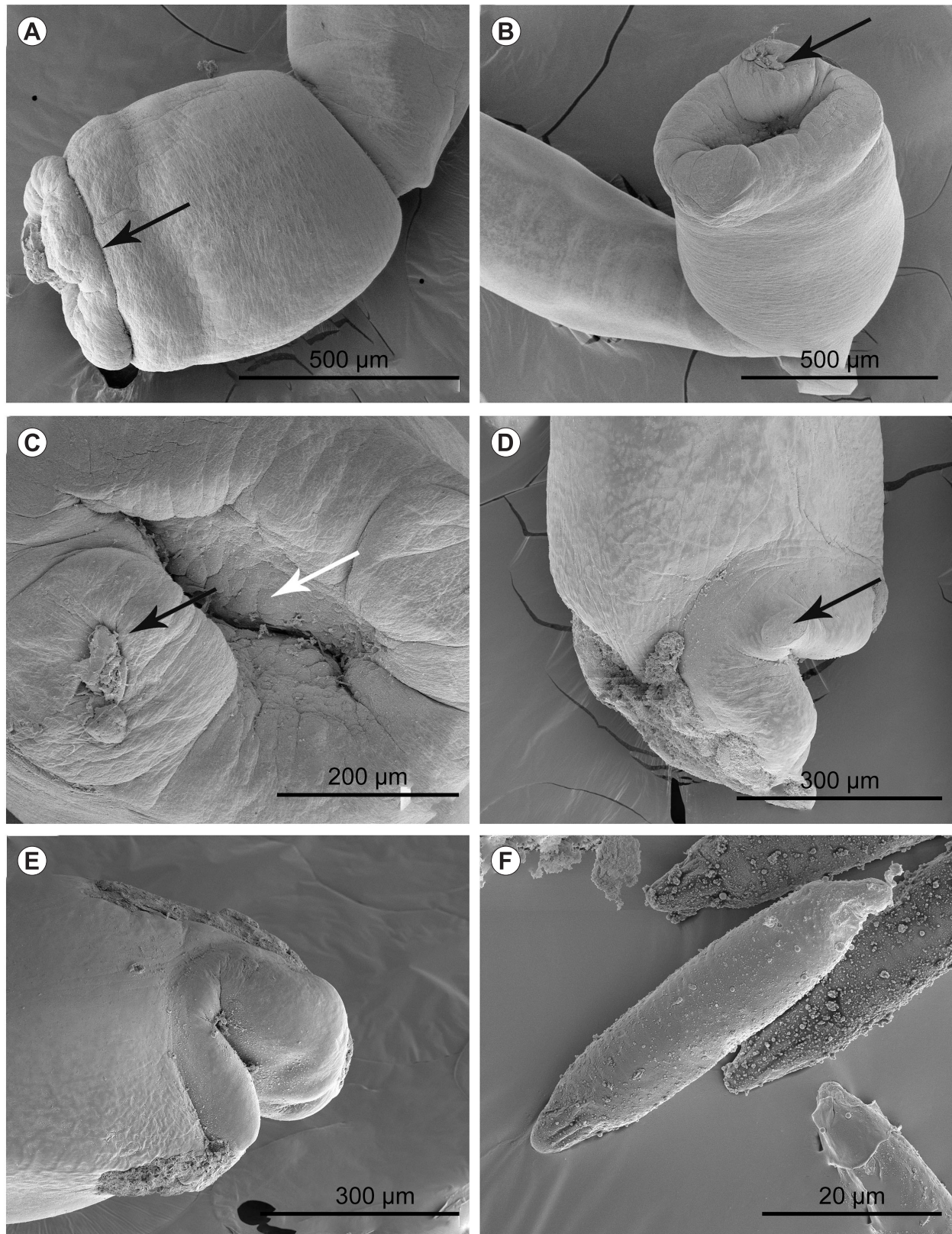
Fig. 4. SEM of specimens of *Illiosentis cetratus* Van Cleave, 1945 from *Menticirrus undulatus* (Girard) in California. **A** – lateral view of bursa showing the distal constriction (arrow); **B** – lateroventral view of the same bursa in Fig. 4A showing the thick lip and the occasional enlarged section (arrow); **C** – higher magnification of the ventral side of the bursa of another specimen with a black arrow pointing to the centre of the enlarged section. A circle of small ovoid sensory papillae appears on the inside of the bursa just below the inner lip side (white arrow); **D** – lateral view of the posterior end of a female specimen showing the arching extension of the dorsal body wall (left) and a large round sensory plate (arrow); **E** – lateral view of the thick ventral genital orifice of a female; **F** – egg. Note the circular ring pattern throughout.
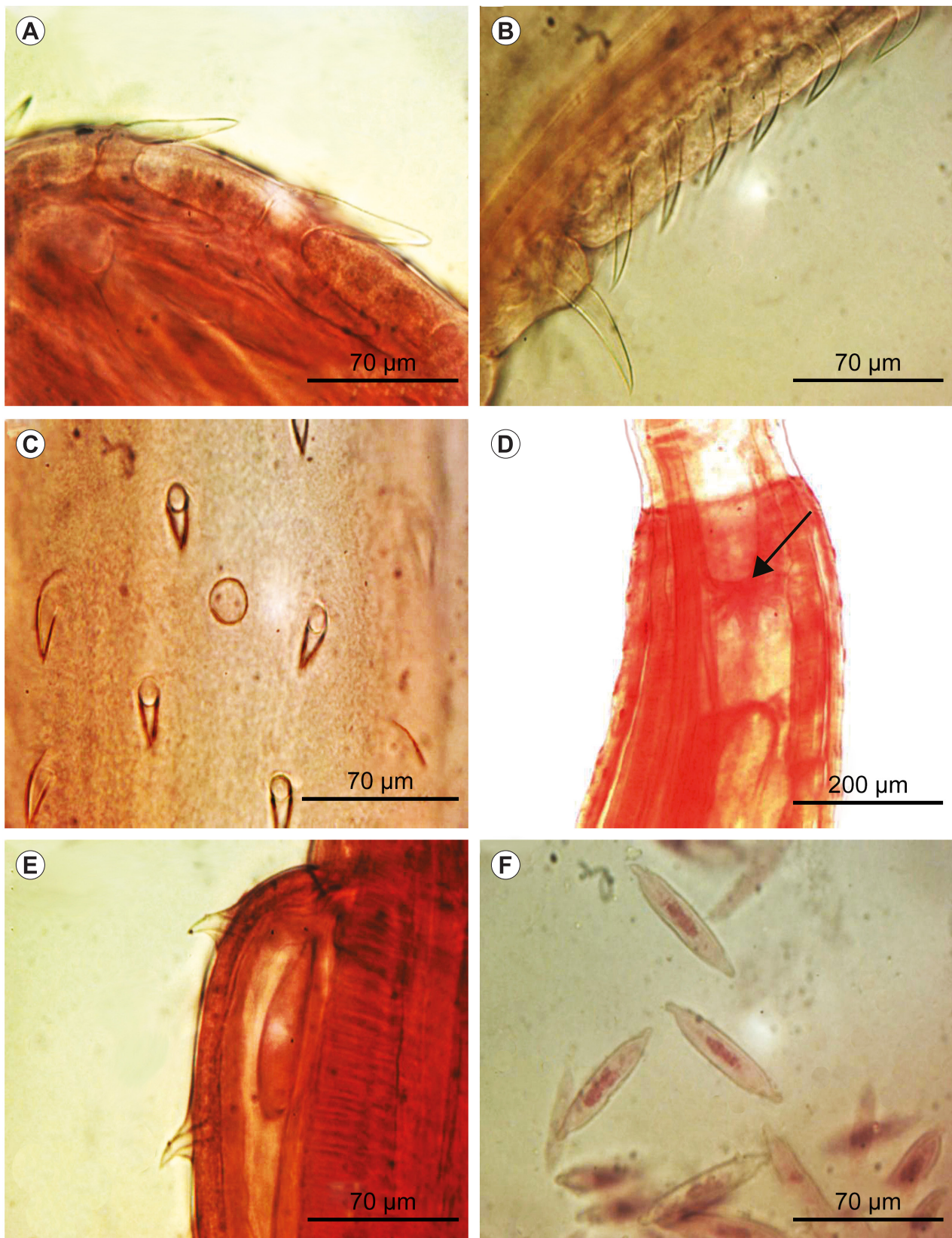
Fig. 5. Light microscope images of specimens of *Illiosentis cetratus* Van Cleave, 1945 from *Menticirrus undulatus* (Girard) in California. **A** – anterior subapical hooks and roots of a male proboscis; **B** – posterior ventral hooks of the proboscis in Fig. 5A; **C** – sensory papilla between hooks 7 and 8 from posterior of a female proboscis; **D** – the anterior portion of a male specimen showing the cephalic ganglion (arrow) and its neurological branches just below the anterior margin of the trunk; **E** – a lateral view of anterior trunk spines showing their rod cores; **F** – eggs released from the body cavity of a punctured gravid female. The marked polar prolongation of the fertilisation membrane is evident. The outer shell is thin and transparent and can barely be seen.
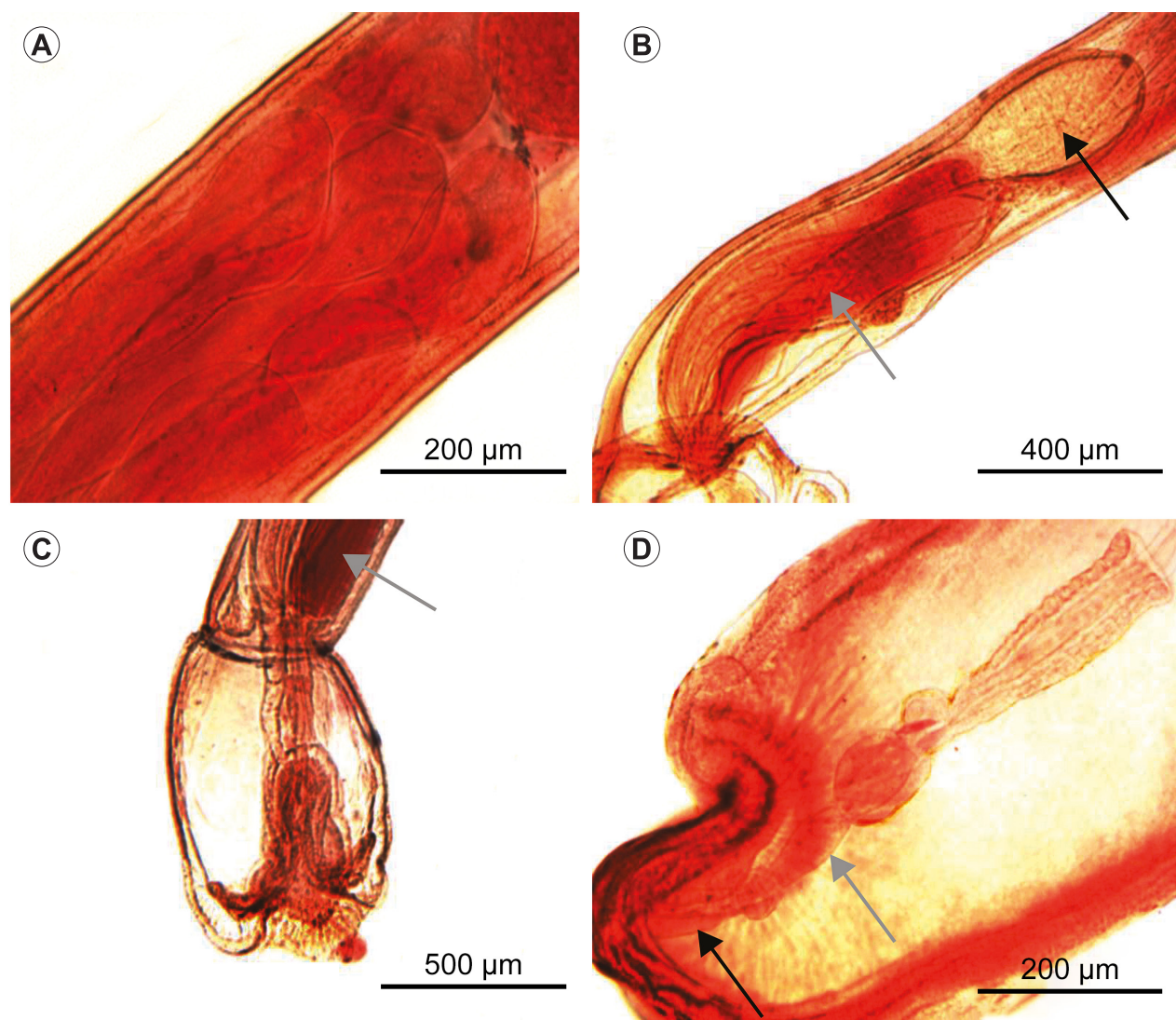
Fig. 6. Detail of the male and female reproductive systems of *Illiosentis cetratus* Van Cleave, 1945 from *Menticirrus undulatus* (Girard) in California seen by light microscopy. **A** – eight cement glands of a male specimen; note the anterior staggering of the distal ends posterior to the testis (upper right corner); **B** – the posterior end of the reproductive system of male showing the dorsal anteriorly ovoid Saefftigen's pouch (black arrow) and its posterior extension partially overlapping the ventral cement gland ducts (gray arrow) all pooling into the bursa; **C** – the bursa and the sperm vesicle (arrow) with the terminal end of reproductive ducts merging around the obscured penis; **D** – lateral view of the reproductive system of a female partially obscured by the fan-shaped muscular organ. Note the envelope surrounding the distal tubular vagina (black arrow) and the short uterus (gray arrow).

Table 4. Chemical composition of whole hooks and spines of specimens of *Illiosentis cetratus* Van Cleave, 1945 from *Menticirrus undulatus* (Girard) in California.

Element*	Apical hook	Middle hook	Posterior hook	Spine
Magnesium (Mg)	**0.14**	**0.36**	**0.20–0.21**	0.16
Sodium (Na)	**0.21**	**0.22**	**0.36–0.38**	0.23
Phosphorous (P)	**0**	**0**	**0–0.03**	0
Sulfur (S)	**2.44**	**6.89**	**7.43–7.52**	0.76
Calcium (Ca)	**0.87**	**0.77**	**0.85–0.87**	0.91

*Palladium (Pd) and Gold (Au) were used to count the specimens and the Gallium for the cross cut of the hooks. These and other elements (C, O, N) common in organic matter are omitted. Data is reported in weight (WT%). Bolded numbers are represented in Fig. 7A–C

of the same hook as well as least concentrations of calcium and phosphorus uncharacteristic of the centre core of hooks. The relative weight % (WT%) concentrations obtained by the TEAM software are reported in Tables 4 and 5. It is worth noting that these reported WT% numbers should not be interpreted as compositional. They are, however, indicative of general differences observed between the selected areas.

Molecular results

New sequences of 18S, 28S rDNA and cox1 were generated from two isolates of *I. cetratus* that showed no intraspecific difference between them. The combined analysis (18S rDNA + 28S rDNA + cox1) of ML and BI tree of species *I. cetratus* showed a resolved relationship in-
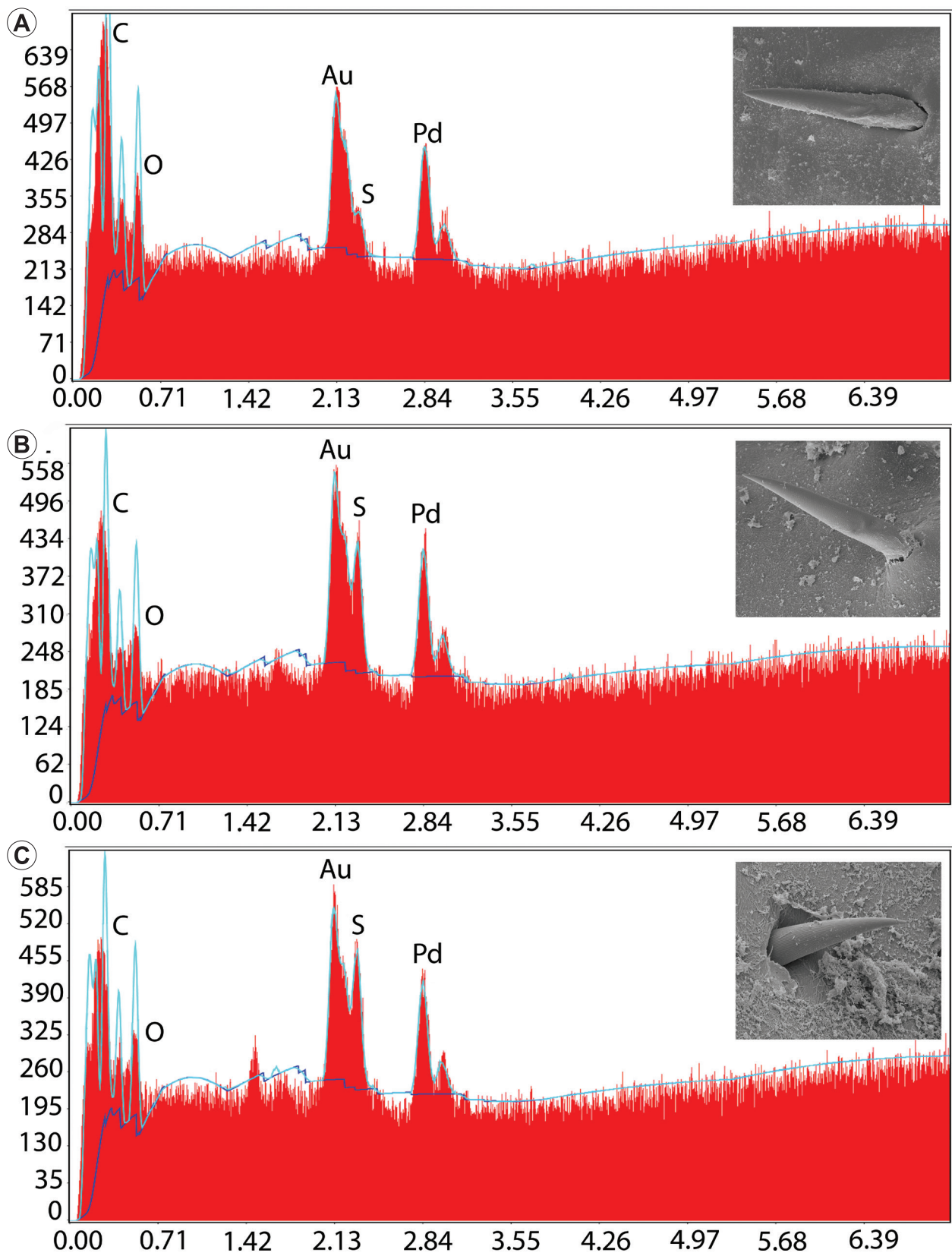
Fig. 7. X-ray panels of elemental scans of hooks of *Illiosentis cetratus* Van Cleave, 1945. See Table 1 for % weight of depicted elements. **A** – scan of whole apical hook. Note a higher level of sulfur compared to the lower levels of phosphorus, magnesium, and calcium. Inset: anterior hook; **B** – scan of whole middle hook. Note the higher level of sulfur compared to anterior hook and the low levels of all other elements. Inset: middle hook; **C** – scan of whole posterior hook. Note the highest level of sulfur and the consistently low level of all other elements. Inset: posterior hook.
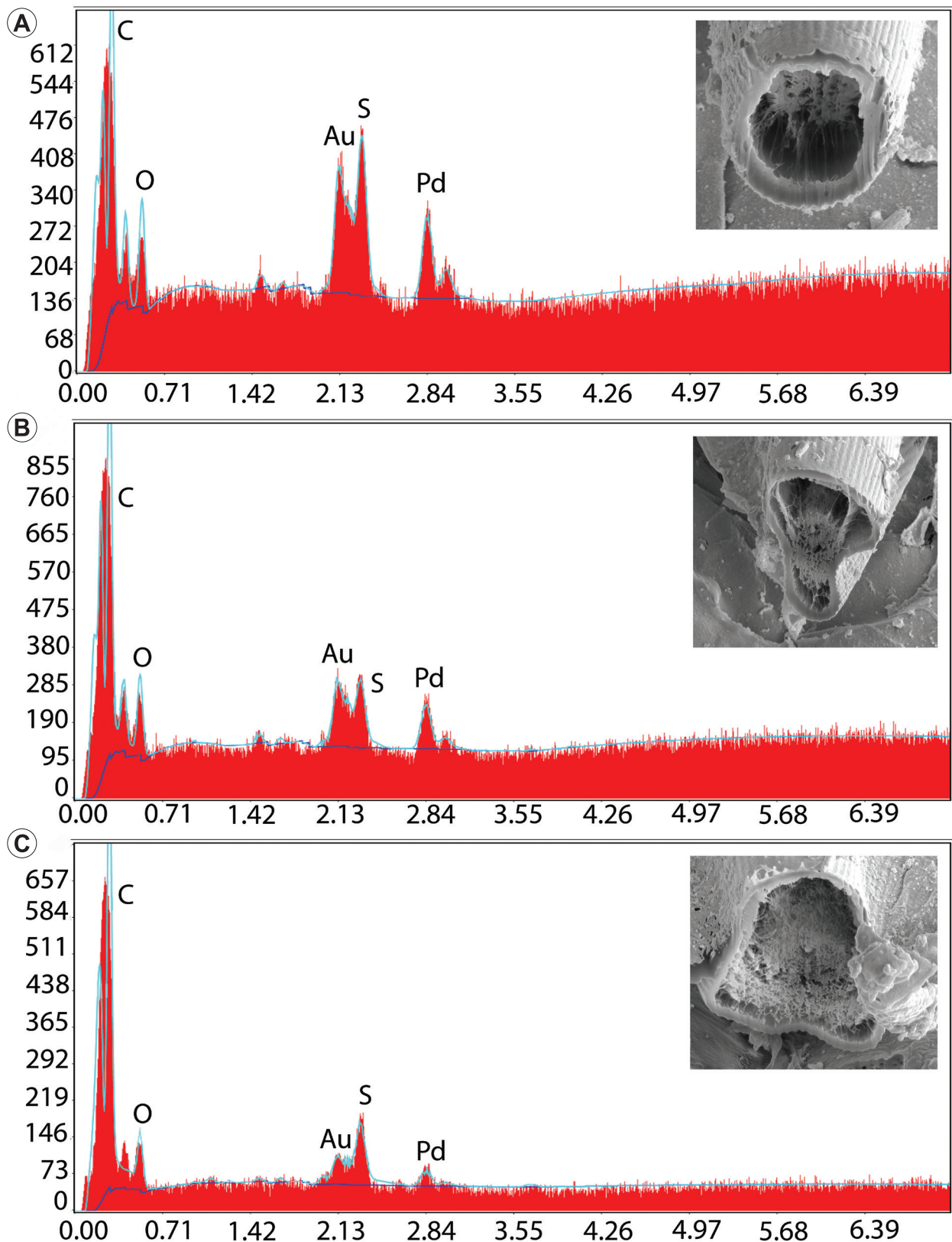
Fig. 8. X-ray panels of elemental scans of various parts of anterior proboscis hooks of *Illiosentis cetratus* Van Cleave, 1945 in sections. See Table 2 for % weight of depicted elements. **A** – scan of the tip of anterior hook. Note the highest level of sulfur compared to the considerably lower levels of sodium, phosphorus, magnesium, and calcium. Inset: cross section of tip of anterior hook; **B** – scan of the middle of anterior hook. Note the higher level of sulfur compared to the low levels of all other elements. Inset: cross section of the middle of anterior hook; **C** – scan of the base of anterior hook. Note the consistently highest level of sulfur compared to the lowest level of all other elements. Inset: cross section of the base of anterior hook.
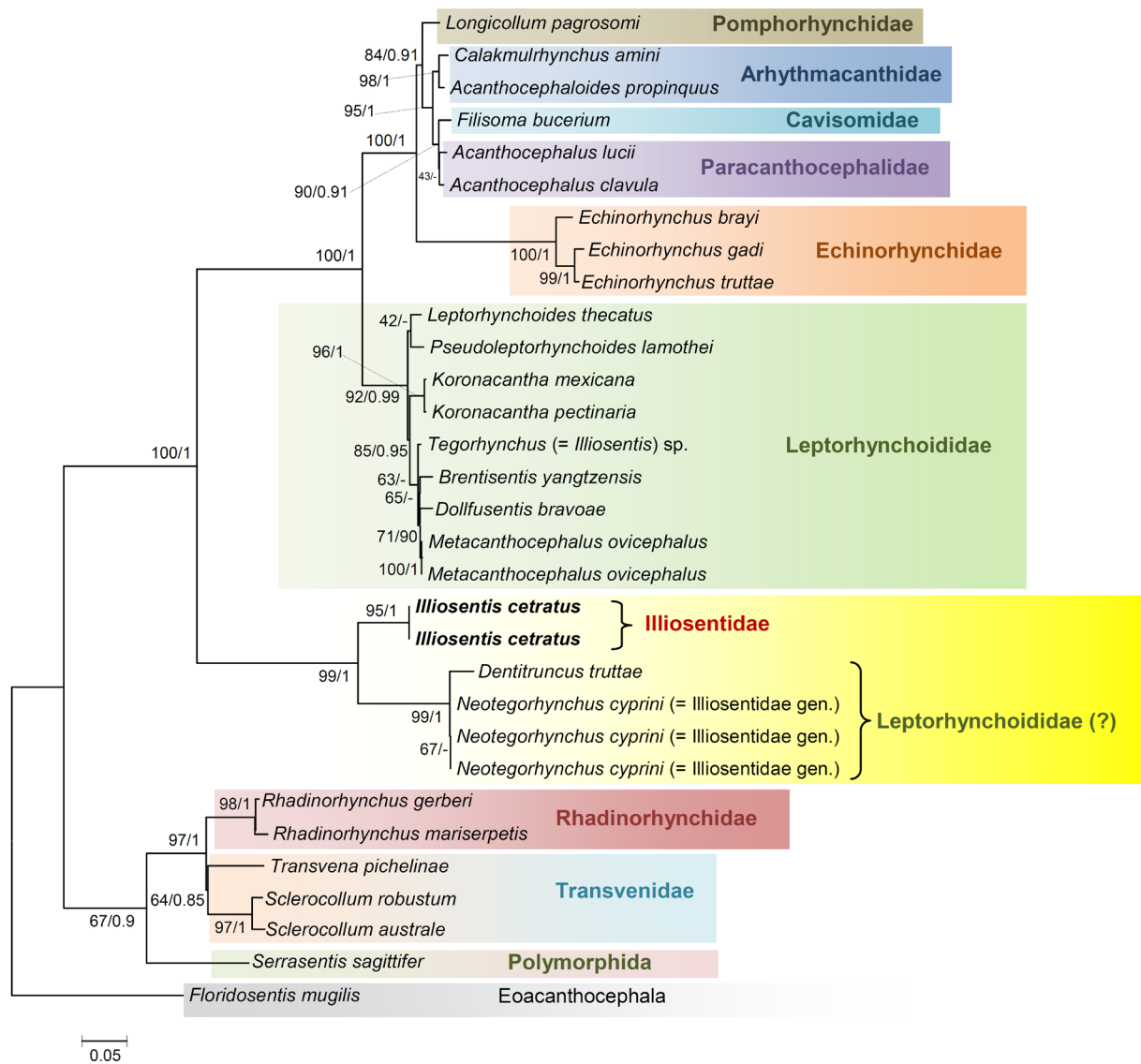
Fig. 9. Phylogenetic tree generated based on three genes 18S rDNA, 28S rDNA and Cox 1 of *Illiosentis cetratus* Van Cleave, 1945 obtained in the present study along with the sequences of species of Leptorhynchoididae available in GenBank. Numbers represented along the nodes indicate ML and BI values respectively. BI posterior probability unsupported values are denoted by hyphens. Species studied in the present study are shown in bold. The scale-bars indicate the number of substitutions per site. GenBank Accession numbers follow each taxon.

Table 5. Chemical localization of elements in various hook parts of specimens of *Illiosentis cetratus* Van Cleave, 1945 from *Menticirrus undulatus* (Girard) in California.

Element*	Anterior hook			Middle	hook
	Tip	Middle	Base	Tip	Center
Magnesium (Mg)	**0.22**	**0.18**	**0.29**	0.32	0.29
Sodium (Na)	**0.25**	**0.07**	**0.22**	0.15	0.10
Phosphorous (P)	**0.32**	**0.54**	**0.95**	0.38	0.45
Sulfur (S)	**11.85**	**6.88**	**9.02**	15.40	8.53
Calcium (Ca)	**0.84**	**0.65**	**0.97**	0.92	0.96

*Palladium (Pd) and Gold (Au) were used to count the specimens and the Gallium for the cross cut of the hooks. These and other elements (C, O, N) common in organic matter are omitted. Data is reported in weight (WT%). Bolded numbers are represented in Fig. 8A–C.

cluding the genera *Dentitruncus* Sinzar, 1955 and *Neotegorhynchus*, clustered in a highly supported clade (99% of ML and 1.00 of BI values) (Fig. 8). On the other hand, the genera *Metacanthocephalus* Yamaguti, 1959, *Dollfusentis*, *Brentisentis* Leotta, Schmidt et Kuntz, 1982, and *Tegorhynchus* were more closely related and comprised various other subclades (Fig. 8). Species of *Koronacantha* Monks et Pérez-Ponce de Léon, 1996 clustered together with strong support, which constituted a sister group with other species of Leptorhynchoididae (Fig. 8). In the tree, *Leptorhynchoides thecatus* (Linton, 1891) and *Pseudoleptorhynchoides lamothei* Salgado-Maldonado, 1976 also shared the same clade as sister-taxon, showed poor resolved relationship with 42% ML values and unsupported BI values (Fig. 8). Our *Illiosentis* species (*I. cetratus*) clade is clearly distinct from the other species of Leptorhynchoididae, es-

Table 6. Acanthocephalan species information used for the phylogenetic analysis based on the combined 18S, 28S rDNA and mt cox1 gene sequences. An asterisk shows unpublished status of sequences on GenBank database.

Taxon	GenBank accession no. 18S	GenBank accession no. 28S	GenBank accession no. mt cox1	References
Palaeacanthocephala				
Longicollum pagrosomi	KX641270	LC195888	KY490048	Hong and Park 2017* for 18S; Mekata et al. 2016* for 28S; Li et al. 2017 for mt cox1
Calakmulrhynchus amini	EU732662	EU732661	-	García-Varela and Andrade-Gómez 2021
Acanthocephaloides propinquus	AY830149	AY829100	DQ089713	García-Varela and Nadler 2005 for 18S and 28S; García-Varela and Nadler 2006 for mt cox1
Filisoma bucerium	AY829110	AF064814	DQ089722	García- Varela et al. 2000 for 18S; García-Varela and Nadler 2005 for 28S; García-Varela and Nadler 2006 for cox1
Acanthocephalus lucii	MW172277	KM656148	MT682949	García-Varela and Andrade-Gómez 2021 for 18S; Wayland et al. 2015 for 28S; Benesh et al. 2006 for mt cox1
Acanthocephalus clavula	MW172278	MW172285	AM039866	García-Varela and Andrade-Gómez 2021 for 18S and 28S; Benesh et al. 2016 for mt cox1
Echinorhynchus brayi	-	KM656151	KP261015	Wayland et al. 2015 for 28S and mt cox1
Echinorhynchus gadi	AY218123	KM656150	KP261022	Giribet et al. 2004 [50] for 18S; Wayland et al. 2015 for 28S and mt cox1
Echinorhynchus truttae	AY830156	KM656147	MN780974	García-Varela and Nadler, 2005 for 18S; Wayland et al. 2015 for 28S; Lewisch et al. 2020 for mt cox1
Leptorhynchoides thecatus	AF001840	AY829093	AY690581	Near et al. 1998 for 18S; García-Varela and Nadler 2005 for 28S; Steinauer et al. 2007 for mt cox1
Pseudoleptorhynchoides lamothei	EU090950	EU090951	EU090949	García-Varela and González-Oliver 2008
Koronacantha mexicana	AY830157	AY829095	DQ089708	García-Varela and Nadler 2005 for 18S and 28S; García-Varela and Nadler 2006 for mt cox1
Koronacantha pectinaria	AF092433	AY829094	DQ089707	Near et al. 1998 for 18S; García-Varela and Nadler 2005 for 28S; Steinauer et al. 2007 for mt cox1
Tegorhynchus (=*Illiosentis*) sp.	AY830158	AY829092	DQ089705	García-Varela and Nadler 2005 for 18S and 28S; García-Varela and Nadler 2006 for mt cox1
Brentisentis yangtzensis	-	-	MK651258	Song et al. 2019 for mt cox1
Dollfusentis bravoae	MK282759	MK282754	MK294064	Keidel et al. 2019
Metacanthocephalus ovicephalus	LC730868	LC730868	LC730869	Kita et al. 2023
Metacanthocephalus ovicephalus	-	LC730867	LC730870	Kita et al. 2023
Illiosentis cetratus	ON180689	OR166369	ON184030	This study
Illiosentis cetratus	ON180690	OR166425	ON184031	This study
Dentitruncus truttae	JX460866	-	JX460903	Vardić Smrzlić et al. 2013 for 18S and mt cox1
Neotegorhynchus cyprini (= Illiosentidae gen.)	MK411441-MK411443	-	MK411444-MK411446	Lisitsyna et al. 2022 for 18S and mt cox1
Rhadinorhynchus gerberi	MN105739	MN105747	MN104898	Lisitsyna et al. 2019
Rhadinorhynchus mariserpentis	MK014866	MK014867	MK012666	Steinauer et al. 2019
Transvena pichelinae	MN105737	MN105743	MN104896	Lisitsyna et al. 2019
Sclerocollum robustum	MN705832	MN705852	MN692688	Huston et al. 2020
Sclerocollum australe	MN705831	MN705851	MN692686	Huston et al. 2020
Serrasentis sagittifer	MF426933	MF426932	MN692701	Barton et al. 2018 for 18S and 28S; Huston et al. 2020 for mt cox1
Eoacanthocephala (outgroup)				
Floridosentis mugilis	AF064811	AY829102	DQ089723	García-Varela et al. 2000 for 18S; García-Varela and Nadler 2005 for 28S; García-Varela and Nadler 2006 for mt cox1

* References marked with asterisks were unavailable to the present authors.

pecially from the newly named *Brentisentis* and *Tegorhynchus* inferred from a significant bootstrap and posterior probability values.

DISCUSSION

We present a unique situation of a rarely encountered acanthocephalan usually infecting one host species in a very limited geographical area in southern California. The description of *Illiosentis cetratus* was limited in scope but still distinctive. Its complete description herein adds missing information, new morphological features, EDXA chemical analysis of hooks as well as molecular analysis, and SEM and light microscope images revealing features not readily depicted by line drawings. Some data from our material were not in agreement with those of Van Cleave's (1945) account such as the number of proboscis hook rows being mostly 14, which is the characteristic number of rows of another species, *Illiosentis furcatus*, and the posi-

tion of the sensory papillae at the level of hooks 7–9 from posterior compared to Van Cleave's (1945) at hooks 8–14 from posterior. Our specimens and those reported by Van Cleave (1945) come from the same host species, *Menticirrhus undulatus*, and from the same geographical location in southern California.

Our observations led us to conclude that we are dealing with the same species, considering other features in common with Van Cleave's (1945) account including similarities of the anatomy of the organ systems and the proboscis, especially the number of hooks per row, even though Van Cleave (1945) did not distinguish between the two types of hooks, describe the hook roots or measure a whole series of these structures or spines, or most other organs. Our description can further help distinguish *I. cetratus* with 18–24 hooks per row, from the closely related and much more widely distributed species, *I. furcatus* with 26–33 hooks per row and by lacking the genital spines characteristic of

the latter species. A considerably more detailed description of *I. furcatus* is needed. Van Cleave and Lincicome (1939) reported *I. furcatus* in the West Atlantic from Cape Cod in Massachusetts, USA to northern Argentina. Our record from *Sciaena deliciosa* in Peru is new and unusual given its locality and also confirms the proboscis armature formula and other morphological similarities noted by Van Cleave and Lincicome (1939).

Micropores

The micropores of *I. cetratus* are associated with internal crypts and vary in diameter and distribution in different trunk regions corresponding with differential absorption of nutrients. We have reported micropores in a large number of acanthocephalan species (Heckmann et al. 2013) and in a few more since, and demonstrated the tunneling from the tegumental surface into the internal crypts by TEM. Amin et al. (2009) gave a summary of the structural-functional relationship of the micropores in various acanthocephalan species. Wright and Lumsden (1969) and Byram and Fisher (1973) reported that the peripheral canals of the micropores are continuous with canalicular crypts. These crypts appear to "constitute a huge increase in external surface area ... implicated in nutrient up take."

Whitfield (1979) estimated a 44-fold increase at a surface density of 15 invaginations per 1 μm² of *Moniliformis moniliformis* (Bremser, 1811) tegumental surface. The micropores and the peripheral canal connections to the canaliculi of the inner layer of the tegument were demonstrated by transmission electron micrographs in *Corynosoma strumosum* (Rudolphi, 1802) from the Caspian seal *Pusa caspica* (Gmelin) in the Caspian Sea (figs. 19, 20 of Amin et al. 2011) and in *Neoechinorhynchus personatus* Tkach, Sarabeev et Shvetsova, 2014 from *Mugil cephalus* Linnaeus in Tunisia (figs. 26, 29, 30 in Amin et al. 2020).

Energy Dispersive X-ray Analysis (EDXA)

Our studies of acanthocephalan worms have usually involved X-ray scans (EDXA) of FIB-sectioned hooks and spines (Heckmann 2006, Heckmann et al. 2007, 2012a, Standing and Heckmann 2014). Hooks (Table 4, Fig. 7) and spines (Table 5, Fig. 8) are evaluated for chemical ions with sulfur (S), calcium (Ca) and phosphorus (P) being the prominent elements. Sulfur is usually seen at the outer edge of large hooks and calcium and phosphorus are major ions in the base and middle of hooks where tension and strength are paramount for hook function.

Results of the X-ray analysis of the FIB-sectioned hooks (dual beam SEM) of *I. cetratus* shows the edge of the anterior hook tip of *I. cetratus* with highest level of sulfur (11.85%) and low levels of calcium (0.84%) and phosphorus (0.32%). The tip of the middle hook had even a higher level of sulfur (15.40%) (Table 5). Middle and posterior whole hooks had considerably higher sulfur levels (6.89% and 7.43–7.52%) than whole apical hooks (2.44%) (Table 4), Those levels are considerably lower than those observed in other species of acanthocephalans but, nevertheless, they are species-specific for *I. cetratus*. For instance, *Cavisoma magnum* (Southwell, 1927) from

M. cephalus in the Arabian Sea, has a similar pattern but considerably higher levels of sulfur in hook tips (43.51%) and edges (27.46%) (Amin et al. 2018). This element (sulfur) is part of the prominent outer layer of most acanthocephalan hooks and is a major contributor of the hardening process. Our results are comparable to those of mammalian teeth enamel.

The centre and base of hooks of the same worms had relatively high sulfur levels but negligible levels of all other metals as the case in all other hooks and hook parts (Tables 4, 5). This is unusual as phosphorus and calcium, the two other essential elements for hook structure (Amin et al. 2018), were not prominent. All chemical elements present in the hooks are typical for acanthocephalans (Heckmann et al. 2007, 2012a,b).

The EDXA appears to be species-specific as in finger prints and is shown to have significant diagnostic value in acanthocephalan systematics. For example, *Moniliformis cryptosaudi* Amin, Heckmann, Sharifdini et Albayati, 2019 from Iraq is morphologically identical to *Moniliformis saudi* Amin, Heckmann, Mohammed et Evans, 2016 from Saudi Arabia, and it was erected based primarily on its distinctly different EDXA pattern (Amin et al. 2019) as a cryptic species. Our methodology for the detection of the chemical profile of hooks in the Acanthocephala has also been used in other parasitic groups, including the Monogenea (Rubtsova et al. 2018, Rubtsova and Heckmann 2019) and Cestoda (Rubtsova and Heckmann 2020).

Amin et al. (2022) discussed in detail the biological significance of EDXA as a diagnostic tool exemplified by the observation that populations of an acanthocephalan species will consistently have similar EDXA spectra irrespective of host species or geography The taxonomic identity of species is deep-seated at the genetic level which is expressed by the organism's morphology and biochemistry as revealed, in part, by its elemental spectra (Amin et al. 2022).

Metal analysis of hooks has become the diagnostic standard since hooks have the highest level of elements compared to the mid- and posterior trunk regions of the acanthocephalan body (Heckmann et al. 2012b). Specifically, the sulfur content in the proboscis is paramount in the composition of disulfide bonds in the thiol groups for cysteine and cystine of the polymerised protein molecules (Stegman 2005). The formed disulfide bonds are direct by-products of the DNA-based process of protein synthesis which makes up the identity of a biological species.

Accordingly, the level of sulfur in our EDXA profiles will indicate the number of sulfur bonds that along with the levels of calcium phosphates, will characterise the identity of a species. Variations in chemical compositions probably indicate differences in allele expression. The sulphide bonds evident in our EDXA profiles have an important role in the stability and rigid nature of the protein accounting for the high sulfur content of the proboscis (Heckmann et al. 2012b). The above processes explain the observed species-specific nature of EDXA profiles noted in our many findings.

Molecular analyses

A combination of morphological and molecular tools for the identification, classification, and estimation of phylogenetic relationships for the species of acanthocephalan is widely applied nowadays and considered to be a very useful approach (García-Varela et al. 2002, Lisitsyna et al. 2019, García-Varela and Andrade-Gómez 2021, Amin et al. 2022, Kita et al. 2023). Before the present study, the position of *I. cetratus* in the Echinorhynchida was not known on a molecular basis. Interestingly, the genus *Illiosentis* was previously placed in the family Rhadinorhynchidae (Van Cleave and Lincicome 1939), but later Golvan (1960) adopted the idea of erecting a new family to accommodate the genus and so he created Illiosentidae. Previous phylogenetic studies proved that the genus *Leptorhynchoides* is more closely related to the different genera of the family Illiosentidae, with which we and other authors also agree (García-Varela and Nadler 2005, García-Varela and González-Oliver 2008, Song et al. 2019). This dispute regarding the various genera of the Illiosentidae continues, and recently molecular markers conveying robust phylogenetic relationships that are required to resolve their status have been use for speicies of the Illiosentidae.

In a previous study of Echinorhynchida, the family Illiosentidae included the species of the genera *Leptorhynchoides* Kostylev, 1924, *Illiosentis*, *Dentitruncus*, and *Koronacantha* (García-Varela and Andrade-Gómez 2021). Recently, in a study by Song et al. (2019), *Brentisentis yangtzensis* Yu et Wu (1989) (Illiosentidae) and *Leptorhynchoides thecatus* (Rhadinorhynchidae) were found to be close relatives and form a sister clade, demonstrating a comparatively close relationship between the Illiosentidae and the Rhadinorhynchidae. Subsequently, a study that included species of eight genera, namely *Brentisentis*, *Dentitruncus*, *Dollfusentis*, *Koronacantha*, *Leptorhynchoides*, *Neotegorhynchus*, *Pseudoleptorhynchoides* Salgado-Maldonado, 1976, *Tegorhynchus* (= *Illiosentis*), and *Metacanthocephalus*, was nested within a clade and indicated Illiosentidae as a junior synonym of Leptorhynchoididae (see Kita et al. 2023).

The resulting combined phylogenetic analysis in our study represented almost the same results as Kita et al. (2023), except for the position of *Dentitruncus truttae* Sinzar, 1955, *Neotegorhynchus cyprini* Lisitsyna, Xi, Orosová, Barčák et Oros, 2022 (= Illiosentidae gen. sp. and *I. cetratus*, which was included for the first time in the current study. The present analyses also showed that *D. truttae* is nested close to *Illiosentis* sp., as also observed by previous researchers (Braicovich et al. 2014, García-Varela and Andrade-Gómez 2021) but neither of them unambiguously established species under Illiosentidae or Leptorhynchoididae. Golvan (1969) discriminated between Illiosentidae and Leptorhynchoididae by the presence or absence of trunk spines, present in Illiosentidae and absent in Leptorhynchoididae.

Phylogenetic analysis generated by Kita et al. (2023) represented that species having trunk spines, i.e., *N. cyprini*, *B. yangtzensis*, *Tegorhynchus* (= *Illiosentis*) sp., *Dentitruncus truttae* Sinzar, 1955, *Dollfusentis bravoae* Salgado-Maldonado, 1976, *Koronacantha mexicana* Monks et Ponce de León, 1996, and *Koronacantha pectinaria* (Van Cleave, 1940), did not show a monophyletic group with which we also agree.

Our species, *I. cetratus*, indicates the existence of two major clades: it has placed itself with other sister taxa, *D. truttae,* and *N. cyprini*, all of which comprise trunk spines. Status of *D. truttae* and *N. cyprini* within Leptorhynchoididae is not certain in the present analysis. Therefore, at this point, we do not agree with Kita et al. (2023) in regard to Illiosentidae being a junior synonym of Leptorhynchoididae, with the conclusion that the family Illiosentidae should not be considered a junior synonym of Leptorhynchoididae. The lack of genomic information on this group (Leptorhynchoididae/Illiosentidae) of species persists; hence, their topology should be inferred with some caution. More studies and species sequences for this group (Leptorhynchoididae/Illiosentidae) are prerequisites to expanding a clear understanding of the phylogenetic relationships between them. Overall, in future studies, validation of this group (Leptorhynchoididae/Illiosentidae) requires a taxonomic revision with more sequences of multiple gene markers from the members of the other genera within these families. This will be important to validate their taxonomic status and systematics.

REFERENCES

Amin O.M. 1985: Classification. In: D.W.T. Crompton and B.B. Nickol (Eds.), Biology of the Acanthocephala. Cambridge University Press, Cambridge, pp. 27–72.

Amin O.M. 2013: Classification of the Acanthocephala. Folia Parasitol. 60: 273–305.

Amin O.M., Ahmed M., Chaudhary A., Anderson Heckmann R., Shanker Singh H. 2022: The morphological and molecular description of *Neoechinorhynchus* (*Neoechinorhynchus*) *poonchensis* sp. n. from *Schizothorax richardsonii* (Gray) in Poonch, Jammu and Kashmir, India. Folia Parasitol. 69: 001.

Amin O.M., Evans P., Heckmann R.A., El-Naggar A.M. 2013: The description of *Mediorhynchus africanus* n. sp. (Acanthocephala: Gigantorhynchidae) from galliform birds in Africa. Parasitol. Res. 112: 2897–2906.

Amin O.M., Heckmann R.A., Bannai M. 2018: *Cavisoma magnum* (Cavisomidae), a unique Pacific acanthocephalan redescribed from an unusual host, *Mugil cephalus* (Mugilidae), in the Arabian Gulf, with notes on histopathology and metal analysis. Parasite 25: 5.

Amin O.M., Heckmann R.A., Halajian A., El-Naggar A.M. 2011: The morphology of a unique population of *Corynosoma strumosum* (Acanthocephala, Polymorphidae) from the Caspian seal, *Pusa caspica*, in the land-locked Caspian Sea using SEM, with special notes on histopathology. Acta Parasitol. 56: 438–445.

Amin O.M., Heckmann R.A., Radwan N.A., Mantuano J.S., Alcivar M.A.Z. 2009: Redescription of *Rhadinorhynchus ornatus* (Acanthocephala: Rhadinorhynchidae) from skipjack tuna, *Katsuwonus pelamis*, collected in the Pacific Ocean off South America, with special reference to new morphological features. J. Parasitol. 95: 656–664.

Amin O.M., Heckmann R.A., Sharifdini M., Albayati N.Y. 2019: *Moniliformis cryptosaudi* n. sp. (Acanthocephala: Moniliformidae) from the long-eared hedgehog *Hemiechinus auratus* (Gmelin) (Erinaceidae) in Iraq; a case of incipient cryptic speciation related to *M. saudi* in Saudi Arabia. Acta Parasitol. 64: 195–204.

Amin O.M., Heckmann R.A., Sharifdini M., Rubtsova N., Chine H.J. 2020: On the *Neoechinorhynchus agilis* (Acanthocephala: Neoechinorhynchidae) complex, with the description of *Neoechinorhynchus ponticus* n. sp. from *Chelon auratus* Risso in the Black Sea. Parasite 27: 48.

Barton D.P., Smales L., Morgan J.A.T. 2018: A redescription of *Serrasentis sagittifer* (Rhadinorhynchidae: Serrasentinae) from *Rachycentron canadum* (Rachycentridae) with comments on its biology and its relationship to other species of *Serrasentis*. J. Parasitol. 104: 117–132.

Benesh D.P., Hasu T., Suomalainen L.R., Valtonen E.T., Tiirola M. 2006: Reliability of mitochondrial DNA in an acanthocephalan: the problem of pseudogenes. Int. J. Parasitol. 36: 247–254.

Braicovich P.E., Lanfranchi A.L., Farber M.D., Marvaldi A.E., Luque J.L., Timi J.T. 2014: Genetic and morphological evidence reveals the existence of a new family, genus and species of Echinorhynchida (Acanthocephala). Folia Parasitol. 61: 377–384.

Bullock W.L., Mateo E. 1970: A reconsideration of the acanthocephalan genera: *Telosentis*, *Illiosentis*, and *Tegorhynchus* on the basis of the type specimens. J. Parasitol. 56: 41–42.

Byram J.E., Fisher F.M.Jr. 1973: The absorptive surface of *Moniliformis dubius* (Acanthocephala). 1. Fine structure. Tissue Cell 5: 553–579.

Darriba D., Taboada G.L., Doallo R., Posada D. 2012: jModelTest 2: more models, new heuristics and parallel computing. Nat. Methods 9: 772.

Folmer O., Black M., Hoeh W., Lutz R., Vrijenhoek R. 1994: DNA primers for amplification of mitochondrial cytochrome c oxidase subunit I from diverse metazoan invertebrates. Mol. Mar. Biol. Biotechnol. 3: 294–299.

García-Varela M., Andrade-Gomez L. 2021: First step to understand the systematics of Echinorhynchidae Cobbold, 1876 (Acanthocephala), inferred through nuclear gene sequences. Parasitol. Int. 81: 102264.

García-Varela M., Cummings M.P., Pérez-Ponce de León G., Gardner S.L., Laclette J.P. 2002: Phylogenetic analysis based on 18S ribosomal RNA gene sequences supports the existence of class Polyacanthocephala (Acanthocephala). Mol. Phylogenet. Evol. 23: 288–292.

García-Varela M., González-Oliver A. 2008: The systematic position of *Leptorhynchoides* (Kostylew, 1924) and *Pseudoleptorhynchoides* (Salgado-Maldonado, 1976), inferred from nuclear and mitochondrial DNA gene sequences. J. Parasitol. 94: 959–962.

García-Varela M., Nadler S.A. 2005: Phylogenetic relationships of Palaeacanthocephala (Acanthocephala) inferred from SSU and LSU rDNA gene sequences. J. Parasitol. 91: 1401–1409.

García-Varela M., Nadler S.A. 2006: Phylogenetic relationships among Syndermata inferred from nuclear and mitochondrial gene sequences. Mol. Phylogenet. Evol. 40: 61–72.

García-Varela M., Pérez-Ponce de León G., De La Torre P., Cummings M.P., Sarma S.S., Laclette J.P. 2000: Phylogenetic relationships of Acanthocephala based on analysis of 18S ribosomal RNA gene sequences. J. Mol. Evol. 50: 532–540.

Giribet G., Sorensen M.V., Funch P., Kristensen R.M., Sterrer W. 2004: Investigations into the phylogenetic position of Micrognathozoa using four molecular loci. Cladistics 20: 1–13.

Golvan Y.J. 1955: Une espèce et une variété nouvelles d'acanthocéphales parasites des poissons de mer des côtes du Sénégal, et redescription de *Serrasentis socialis* (Leidy 1851) Van Cleave 1924. Ann. Parasitol. Hum. Comp. 31: 225–241.

Golvan Y.J. 1960: Le phylum des Acanthocephala. Troisième note. La classe des Palaeacanthocephala (Meyer 1931) (à suivre). Ann. Parasitol. Hum. Comp 35: 138–165.

Golvan Y.J. 1969: Systématique des acanthocéphales (Acanthocephala Rudolphi 1801). Première partie. L'ordre des Palaeacanthocephala Meyer 1931. Premier fascicule. La super-famille des Echinorhynchoidea (Cobbold 1876) Golvan et Houin 1963. Mém. Mus. Nat. d'Hist. Nat. (Paris), Sér. A, Zool., Nouvelle Sér. 57: 1–373.

Golvan Y.J. 1994: Nomenclature of the Acanthocephala, Res. Rev. Parasitol. 54: 135–205.

Heckmann R.A. 2006: Energy dispersive x-ray analysis (EDXA) in conjunction with electron optics, a tool for analyzing aquatic animal parasite diseases and deaths, an update. Proc. Parasitol. 41: 1–18.

Heckmann R.A., Amin O.M., El Naggar A.M. 2013: Micropores of Acanthocephala, a scanning electron microscopy study. Sci. Parasitol. 14: 105–113.

Heckmann R.A., Amin O.M., Radwan N.A.E., Standing M.D., Eggett D.L. 2012b: Comparative chemical element analysis using energy dispersive x-ray microanalysis (EDXA) for four species of Acanthocephala. Sci. Parasitol. 13: 27–35.

Heckmann R.A., Amin O.M., Radwan N.A.E, Standing M.D., Eggett D.L., El Naggar A.M. 2012a: Fine structure and energy dispersive X-ray analysis (EDXA) of the proboscis hooks of *Rhadinorhynchus ornatus*, Van Cleave 1918 (Rhadinorhynchidae: Acanthocephala). Sci. Parasitol. 13: 37–43.

Heckmann R.A., Amin O.M., Standing M.D. 2007: Chemical analysis of metals in acanthocephalans using energy dispersive

X-ray analysis (EDXA, XEDS) in conjunction with a scanning electron microscope (SEM). Comp. Parasitol. 74: 388–391.

Huston D.C., Cribb T.H., Smales L.R. 2020: Molecular characterisation of acanthocephalans from Australian marine teleosts: proposal of a new family, synonymy of another and transfer of taxa between orders. Syst. Parasitol. 97: 1–23.

Keidel L., García-Varela M., Brener B., Pérez-Ponce de León G., Santos C.P. 2019: Integrative taxonomy reveals a new species of *Dollfusentis* (Acanthocephala: Illiosentidae), in *Orthopristis ruber* (Osteichthyes: Haemulidae) from Rio de Janeiro, Brazil. Parasitol. Int. 71: 132–142.

Kita Y., Hiruta S.F., Sasaki M., Kajihara H. 2023: Systematic position of the genus *Metacanthocephalus* Yamaguti, 1959 (Palaeacanthocephala: Echinorhynchida) inferred from molecular evidence, with a redescription of *Metacanthocephalus ovicephalus* (Zhukov, 1960). Parasit. Int. 94: 102731.

Lee R.E. 1992: Scanning Electron Microscopy and X-Ray Microanalysis. Prentice Hall, Englewood Cliffs, New Jersey, USA. 458 pp.

Leotta S. H., Schmidt G. D., Kuntz R. E.. 1982: *Brentisentis uncinus* gen. et sp. n. and *Gorgorhynchus satoi* (Morisita, 1937) Yamaguti, 1963 from Taiwan. J. Parasitol. 68: 134–137.

Li L., Yang Y., Zhang L.P. 2017: Morphological and molecular study of *Longicollum pagrosomi* Yamaguti, 1935 (Acanthocephala: Pomphorhynchidae) from the barred knifejaw *Oplegnathus fasciatus* (Temminck and Schlegel) (Perciformes: Oplegnathidae) in the East China Sea. Syst. Parasitol. 94: 255–261.

Lisitsyna O., Kudlai O., Cribb T.H., Smit N.J. 2019: Three new species of acanthocephalans (Palaeacanthocephala) from marine fishes collected off the East Coast of South Africa. Folia Parasitol. 66: 012.

Lisitsyna O., Xi B.W., Orosová M., Barčák D., Oros M. 2022: The erection of a new genus, *Neotegorhynchus* n. g. (Palaeacanthocephala, Illiosentidae), with a redescription of *Neotegorhynchus cyprini* n. comb. from *Cyprinus carpio* from the Yangtze River basin, China. Zootaxa 5150: 83–96.

Milne I., Lindner D., Bayer M., Husmeier D., Mcguire G., Marshall D.F., Wright F. 2008: TOPALi v2: a rich graphical interface for evolutionary analyses of multiple alignments on HPC clusters and multi-core desktops. Bioinformatics 25: 126–127.

Monks S., Pulido-Flores G. 2002: Reevaluation and emended diagnosis of *Illiosentis* and *I. heteracanthus* (Acanthocephala: Illiosentidae). J. Parasitol. 88: 365–369.

Near T.J., Garey J.R., Nadler S.A. 1998. Phylogenetic relationships of the Acanthocephala inferred from 18S ribosomal DNA sequences. Mol. Phylogenet. Evol. 10: 287–298.

Petrochenko V.I. 1956. Acanthocephala of Domestic and Wild Animals. Vol. 1, Moscow, Izdatel'stvo Akademii Nauk SSSR; 435 pp. (English translation by Israel Program for Scientific Translations Ltd., Jerusalem, 1971, 465 pp.)

Rubtsova N.Y., Heckmann R.A. 2019: Structure and morphometrics of *Ancyrocephalus paradoxus* (Monogenea: Ancyrocephalidae) from *Sander lucioperca* (Percidae) in Czechia. Helminthologia 56: 11–21.

Rubtsova N.Y., Heckmann R.A. 2020: Morphological features and structural analysis of plerocercoids of *Spirometra erinaceieuropaei* (Cestoda: Diphyllobothriidae) from European pine marten, *Martes martes* (Mammalia: Mustelidae) in Ukraine. Comp. Parasitol. 87: 109–117.

Rubtsova N.Y., Heckmann R.A., Smit W.S., Luus-Powell W.J., Halajian A., Roux F. 2018: Morphological studies of developmental stages of *Oculotrema hippopotami* (Monogenea: Polystomatidae) infecting the eye of *Hippopotamus amphibius* (Mammalia: Hippopotamidae) using SEM and EDXA with notes on histopathology. Korean J. Parasitol. 56: 463–475.

Song R., Zhang D., Gao J. W., ChengX. F., Xie M., Li H., Wu Y.A. 2019: Characterization of the complete mitochondrial genome of *Brentisentis yangtzensis* Yu and Wu, 1989 (Acanthocephala, Illiosentidae). Zookeys 861: 1–14.

Standing M.D., Heckmann R.A. 2014: Features of acanthocephalan hooks using dual beam preparation and XEDS phase maps. Microsc. Microanal. 20: 1328–1329.

Stegman J. K. 2005: Stedman's Medical Dictionary for the Health Professions and Nursing. Fifth Edition. Lippincott, Williams and Wilkins, Baltimore, 1597 pp.

Steinauer M.L., Garcia-Vedrenne A.E., Weinstein S.B., Kuris A.M. 2019: Acanthocephalan parasites of the oarfish, *Regalecus russelii* (Regalecidae), with a description of a new species of *Gymnorhadinorhynchus* (Acanthocephala: Gymnorhadinorhynchidae). J. Parasitol. 105: 124–132.

Steinauer M.L., Nickol B.B., Orti G. 2007: Cryptic speciation and patterns of phenotypic variation of a highly variable acanthocephalan parasite. Mol. Ecol. 16: 4097–4109.

Suzuki N., Hoshino K., Murakami K., Takeyama H., Chow S. 2008: Molecular diet analysis of phyllosoma larvae of the Japanese spiny lobster *Palinurus japonicus* (Decapoda: Crustacea). Mar. Biotechnol. 10: 49–55.

Tamura K., Stecher G., Kumar S. 2021: MEGA11: Molecular Evolutionary Genetics Analysis Version 11. Mol. Biol. Evol. 38: 3022–3027.

Van Cleave H.J. 1945: A new species of the acanthocephalan genus *Illiosentis* (*Rhadinorhynchus*). J. Parasitol. 31: 57–60.

Van Cleave H.J., Lincicome D.R. 1939: On a new genus and species of Rhadinorhynchidae (Acanthocephala). Parasitology 31: 413–416.

Vardić Smrzlić I., Valić D., Kapetanović D., Dragun Z., Gjurčević E., Ćetković H., Teskeredžić E. 2013: Molecular characterisation and infection dynamics of *Dentitruncus truttae* from trout (*Salmo trutta* and *Oncorhynchus mykiss*) in Krka River, Croatia. Vet. Parasitol. 197: 604–613.

Whitfield P.J. 1979: The Biology of Parasitism: An Introduction to the Study of Associating Organisms. University Park Press, Baltimore, Maryland, 277 pp.

Wright R. D., Lumsden R.D. 1969: Ultrastructure of the tegumentary pore canal system of the acanthocephalan *Moniliformis dubius*. J. Parasitol. 55: 993–1003.

Yamaguti S. 1963: Systema Helminthum, Acanthocephala, New York and London, Interscience Publishers, 423 pp.